J. Fluid Mech. (1995), *vol.* 297, *pp.* 215–230

Numerical study of the oscillations of axially excited liquid annuli with rotational symmetry enclosed in revolving circular cylindrical containers

By M. EHMANN AND J. SIEKMANN
Chair of Mechanics, University GH Essen, 45 117 Essen, Germany

(Received 9 December 1993 and in revised form 30 November 1994)

In this paper we investigate numerically the periodic, axisymmetric response of a liquid annulus enclosed in a revolving cylinder and subject to a periodic axial excitation within the range of the natural frequencies. We use a description which employs as solution variables the transverse component of the vorticity vector, the scalar stream function and the transverse velocity component, as well as the position of the free surface. The acceleration due to gravity is neglected, whereas friction and surface tension are taken into account. At the fixed walls the no-slip condition is fulfilled except at points on the contact line. At the contact line the slip condition is applied. The solution of this problem is achieved using the spectral method in the time direction and finite differences in the space direction, whereby surface-adapted coordinates are utilized. Far away from the walls the computational results show good agreement with results obtained from a linearized theory assuming an inviscid liquid, while at the walls boundary layers are generated.

1. Introduction

Rotating fluids are not only of scientific interest *per se*, but are of importance also in nature and technical applications. Galaxies as well as some planets can be considered as examples of rotating fluids, and the atmosphere and the oceans of the Earth are rotating fluid systems. With respect to technical applications rotating fluids occur in centrifuges, in the hollow shafts of liquid-cooled turbines, in the spin stabilization of rockets, and in zone-melting processes of monocrystal growth.

Rayleigh (1892) determined theoretically the instability limit for the existence of cylindrical bubbles for vanishing volume forces. Experimental studies had already been carried out by Plateau (1873). These experiments were repeated by Mason (1970), who found very good agreement with theoretical results. The stability of rotating menisci, subject to reduced gravity, was investigated by Seebold & Reynolds (1965), who showed under what circumstances defined liquid configurations are possible. In the course of their investigations they also studied the case where the gas volume connects the two solid end plates of a cylindrical container, i.e. an annulus.

Miles (1959) examined the natural oscillations of a liquid with a free surface in a cylindrical tank rotating about the axis of revolution and the response of this configuration to a harmonic excitation perpendicular to the axis of revolution. Miles & Troesch (1961), and Kollmann (1962), published research on the natural oscillations of such systems, applying a linearized inviscid theory and neglecting surface tension. In particular Miles & Troesch demonstrated the existence of radial nodes which occur only if the Coriolis acceleration is taken into consideration. These authors were

interested in the behaviour of liquid-filled rotating rockets while Kollmann studied the oscillatory behaviour in liquid-cooled hollow shafts of gas turbines.

Motivated by the problem of nutational damping of spin-stabilized satellites in orbit, Bauer (1980) studied the oscillations of immiscible fluids in an infinitely long rotating circular cylinder. He employed a non-viscous two-dimensional theory in the (r, ϕ)-plane and neglected surface tension. The eigenfrequency equations and the response of such fluid systems to radial and transverse excitations were calculated. In a subsequent paper, Bauer (1981) extended his analysis, taking into account surface tension in order to predict the occurrence of waves which have a disturbing effect on crystal growth in melts supported by surface tension (interfacial tension). For the equilibrium configuration he gives stability limits and confirms a result reported by Hocking & Michael (1959) for the special case of rotating liquid columns. If viscosity is taken into consideration the stability limits exhibit a different course as shown by Hocking (1960) and Gillis (1961).

Experimental work on the stability of rotating liquid bridges was carried out by Carruthers & Grasso (1972). They determined the maximal stable lengths of such bridges and compared their findings with those of Hocking and Gillis.

Theoretical studies by Bauer (1982*a*, *b*) are devoted to the determination of the natural frequencies of rotating fluid systems in a cylindrical arrangement by applying an inviscid three-dimensional theory with surface tension taken into account. Furthermore, Bauer (1984) calculated the natural damped frequencies of an infinitely long column of immiscible viscous liquids.

The response of liquid systems contained in a closed rotating cylinder spinning about the axis of revolution is the subject of experimental investigations by Chun *et al.* (1987) and Raake (1991). They found excellent agreement between experimentally and analytically determined eigenfrequencies. However, a symmetric deviation with respect to higher eigenvalues was noticed.

Numerical calculations of flows having a free surface were done for the first time by Harlow & Welch (1965). They applied the MAC-method, again neglecting surface tension. A technique for including surface-tension effects was described by Daly (1969). However, an accurate determination of the free surface was not possible because computations were carried out by utilizing a fixed Cartesian coordinate system. This can be remedied by using grids adapted to the surface, e.g. Hirt, Amsden & Cook (1974). Ryskin & Leal (1984) use orthogonal surface-adapted grids which simplified the boundary conditions.

Whereas the methods mentioned hitherto employ finite differences, Balasubramanian (1990) developed a finite element method, using a mixed Euler–Lagrange representation. He studied waves in different geometries, again neglecting surface tension effects.

Veldman & Vogels (1984) dealt with the response of a rotating liquid–gas configuration in a rotating cylindrical vessel under low-gravity conditions and different excitations. They make use of the SOLA-VOF method, described by Hirt & Nichols (1981), assuming an axisymmetric flow field and adding the impulse equation in the transverse direction. For a harmonic excitation with the eigenfrequency they determine the transient state of the configuration and note good agreement with the analytically determined eigenfrequency.

In the present work the behaviour of a liquid with a free surface is investigated. The system is in a periodic state and subject to a periodic excitation. A numerical procedure has been chosen which allows the oscillatory behaviour in the periodic state to be determined without the examination of the transient state. This is accomplished by

application of the spectral method in the time direction and use of the finite difference method in the space direction, employing a surface-adapted unsteady grid. Spectral methods in the space direction have been successfully used in many problems, while the application of this method in the time direction is unusual (Fletcher 1984; Cannuto *et al.* 1988).

In the course of the development of the solution it turned out to be advantageous to apply computer algebra systems such as presented for example in a survey article by van Hulzen & Calmet (1982). In our study the system REDUCE was utilized (cf. also Rayna 1987 and Hearn 1983).

2. Governing equations

Let us consider (figure 1) a cylindrical vessel of height h and radius b enclosing a liquid and a gas. The liquid fills a hollow cylinder of height h, hence the latter has a reduced inner radius r and an outer radius b. The fluid system revolves with a constant angular speed Ω about the axis of revolution of the vessel and, in addition, is subject to an acceleration $A\cos(\Omega_A t)$ in the axial direction, with A the amplitude of the excitation, Ω_A the excitation frequency and t the time. The shape of the generated free liquid surface can be described by the distance $f(z, t)$ from the outer radius of the vessel, where z denotes the axial distance of a cylindrical coordinate system. Furthermore, we suppose that the flow within the vessel is axisymmetric. Provided that the viscosity and the density of the gas are negligible in relation to the material constants of the liquid, the problem under consideration can be simplified by postulating a gas with constant pressure and vanishing viscosity and density.

The liquid is assumed to be incompressible, having a constant density ρ. It is also assumed to be a Newtonian fluid with a constant kinematic viscosity ν. At the interface between the liquid and the gas a surface tension T_{12} acts, which is assumed to be constant over the interface.

In what follows, and with the liquid properties just mentioned, a mathematical model for the treatment of the flow field resulting from excitation in the range of eigenfrequencies (natural frequencies) is presented.

2.1. *Differential equations within the fluid interior*

The Navier–Stokes equations in a rotating reference frame can be written in the form (see e.g. Greenspan 1969)

$$\frac{\partial \boldsymbol{u}}{\partial t}+\tfrac{1}{2}\nabla(\boldsymbol{u}\cdot\boldsymbol{u})+(\nabla\times\boldsymbol{u})\times\boldsymbol{u}+2\boldsymbol{\Omega}\times\boldsymbol{u}+\boldsymbol{\Omega}\times(\boldsymbol{\Omega}\times\boldsymbol{r})=-\frac{1}{\rho}\nabla p+\boldsymbol{F}-\nu\nabla\times(\nabla\times\boldsymbol{u}), \quad (1)$$

where $\boldsymbol{u}$, with components u, v, w in a cylindrical coordinate system $(0; r, \phi, z)$, denotes the velocity vector a fluid particle at the position $\boldsymbol{r}$, $\boldsymbol{\Omega}$ is the constant angular velocity of the rotating coordinate system and p is the pressure. $\boldsymbol{F}$ is a volume force which is generated by the accelerations of the coordinate system. Furthermore $2\boldsymbol{\Omega}\times\boldsymbol{u}$ is the Coriolis acceleration and $\boldsymbol{\Omega}\times(\boldsymbol{\Omega}\times\boldsymbol{r})$ the centrifugal acceleration.

Next the dimensional quantities can be made dimensionless via

$$\boldsymbol{r}=L\boldsymbol{r}^*, \quad \boldsymbol{u}=U\boldsymbol{u}^*, \quad t=\Omega^{-1}t^*, \quad p=\rho\Omega ULp^*, \quad (2)$$

with L (e.g. h) a characteristic length of the configuration, and U a characteristic velocity. Furthermore $\boldsymbol{\Omega}=\Omega\boldsymbol{k}$, with $\boldsymbol{k}$ the unit vector in the direction of the axis of revolution.

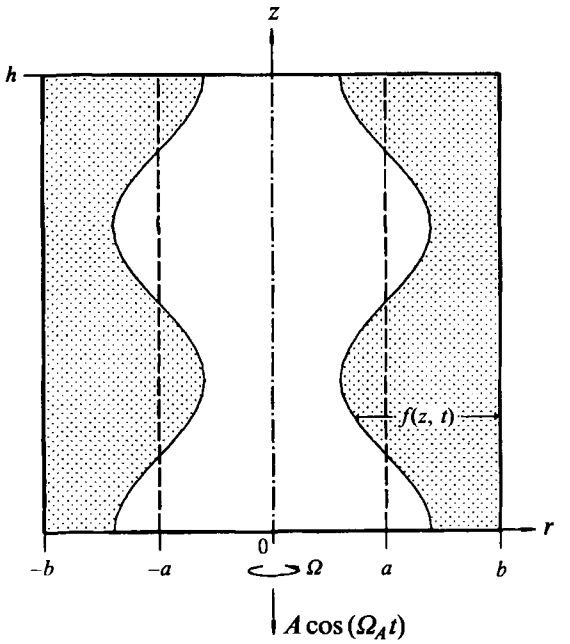

FIGURE 1. Geometry of the rotating fluid system; notation.

Thus

$$\frac{\partial \boldsymbol{u}}{\partial t} + Ro\left[\tfrac{1}{2}\,grad(\boldsymbol{u}\cdot\boldsymbol{u}) + (\operatorname{curl}\boldsymbol{u})\times\boldsymbol{u}\right] + 2\boldsymbol{k}\times\boldsymbol{u} + \boldsymbol{k}\times(\boldsymbol{k}\times\boldsymbol{r})$$

$$= \operatorname{grad} p + \boldsymbol{F} - Ek \operatorname{curl}(\operatorname{curl}\boldsymbol{u}), \quad (3)$$

where the asterisks have been omitted. The dimensionless numbers $Ek = \nu/\Omega L^2$ and $Ro = U/\Omega L$ are the Ekman number and the Rossby number, respectively.

Since the motion of the fluid is determined by a resonance condition, *a priori* there is no characteristic velocity. The latter results from the response behaviour of the liquid only. Hence we postulate $U = \Omega/L$, so that $Ro = 1$. The incompressibility condition yields $\operatorname{div}\boldsymbol{u} = 0$.

As mentioned previously, for the representation of the flow field we employ cylindrical coordinates with axial distance z, radial distance normal to the symmetry axis r, and azimuthal angle ϕ. Because of the assumption that the fluid configuration is axisymmetric, there is no azimuthal dependence of the variables, i.e. for each arbitrary quantity g we have $\partial g/\partial\phi = 0$. Thus the continuity equation reads

$$\frac{\partial u}{\partial r} + \frac{\partial w}{\partial z} + \frac{u}{r} = 0. \quad (4)$$

Applying the curl operator to (3), the pressure can be eliminated and on making use of the vorticity vector $\boldsymbol{\omega} = \operatorname{curl}\boldsymbol{u}$, the vorticity transport equation results. Defining the vector potential $\boldsymbol{\Psi}$ as $\boldsymbol{u} = \operatorname{curl}\boldsymbol{\Psi}$, the continuity equation is satisfied identically. Hence there follows after some standard manipulations

$$\boldsymbol{u} = \left(-\frac{\partial \Psi_\phi}{\partial z}, \frac{\partial \Psi_r}{\partial z} - \frac{\partial \Psi_z}{\partial r}, \frac{\Psi_r}{r} - \frac{\partial \Psi_\phi}{\partial r}\right)^T, \quad (5)$$

where the superscript T denotes the transpose. The vorticity vector reads

$$\boldsymbol{\omega} = \operatorname{curl} \boldsymbol{u} = \left(-\frac{\partial v}{\partial z}, \frac{\partial u}{\partial z} - \frac{\partial w}{\partial r}, \frac{v}{r} + \frac{\partial v}{\partial r} \right)^T. \tag{6}$$

From this we recognize that a mixed representation turns out to be useful by keeping the ϕ-component of the velocity (v) and utilizing the ϕ-components only from the vorticity vector and from the vector potential. Thus the scalar field ω, following from (6), is given by

$$\omega = \frac{\partial u}{\partial z} - \frac{\partial w}{\partial r}. \tag{7}$$

Furthermore it is appropriate to introduce a scalar function ψ (Stokes stream function for axisymmetric flow) given by $\psi = r\Psi_\phi$.

Hence we get for the velocity components u and w the expressions

$$u = -\frac{1}{r}\frac{\partial \psi}{\partial z}, \quad w = \frac{1}{r}\frac{\partial \psi}{\partial r}, \tag{8}$$

From that one obtains:
the ϕ-component of the Navier–Stokes equation

$$r^2\frac{\partial v}{\partial t} - r\frac{\partial \psi}{\partial z}\frac{\partial v}{\partial r} + r\frac{\partial \psi}{\partial r}\frac{\partial v}{\partial z} - (2r+v)\frac{\partial \psi}{\partial z} = Ek\left(r^2\frac{\partial^2 v}{\partial r^2} + r^2\frac{\partial^2 v}{\partial z^2} + r\frac{\partial v}{\partial r} - v \right), \tag{9}$$

the vorticity transport equation

$$-2(r^2+rv)\frac{\partial v}{\partial z} + r\frac{\partial \psi}{\partial r}\frac{\partial \omega}{\partial z} + \frac{\partial \psi}{\partial z}\left(\omega - r\frac{\partial \omega}{\partial r} \right) + r^2\frac{\partial \omega}{\partial t} = Ek\left(r^2\frac{\partial^2 \omega}{\partial z^2} + r^2\frac{\partial \omega}{\partial r^2} + r\frac{\partial \omega}{\partial r} - \omega \right), \tag{10}$$

and the stream function–vorticity equation (resulting from (7) and (8))

$$r^2\omega = \frac{\partial \psi}{\partial r} - r\frac{\partial^2 \psi}{\partial r^2} - r\frac{\partial^2 \psi}{\partial z^2}. \tag{11}$$

2.2. *Boundary conditions*

The no-slip condition at the rotating vessel requires

$$u = -\frac{1}{r}\frac{\partial \psi}{\partial z} = 0, \quad v = 0, \quad w = \frac{1}{r}\frac{\partial \psi}{\partial r} = 0. \tag{12a, b, c}$$

If we put $\psi = 0$ at the fixed walls, we see that (12a, c) are fulfilled. Referring to the stream function–vorticity (11) and the boundary conditions (12a, c), we find at the upper and lower solid plates

$$\omega = -\frac{1}{r^2}\frac{\partial^2 \psi}{\partial z^2} \quad \text{at} \quad z = 0 \quad \text{and} \quad z = 1, \tag{13}$$

whilst in the lateral area we obtain

$$\omega = -\frac{1}{r}\frac{\partial^2 \psi}{\partial r^2} \quad \text{at} \quad r = b. \tag{14}$$

At the free liquid surface (liquid–gas interface)

$$r = b - f \tag{15}$$

we assume impermeability. Now for a moving surface we can write $\boldsymbol{n}\cdot(\boldsymbol{u}-\boldsymbol{w})=0$ (see, e.g. Becker & Bürger 1975) if the free surface is considered as a surface of discontinuity. In this equation the unit normal vector (pointing in the direction out of the liquid) is given by

$$\boldsymbol{n}=\frac{-1}{[1+(\partial f/\partial z)^2]^{1/2}}\left(1,0,\frac{\partial f}{\partial z}\right)^T, \tag{16}$$

and the velocity vector of the free surface is

$$\boldsymbol{w}=\left(-\frac{\partial f}{\partial t},\quad 0,0\right)^T. \tag{17}$$

The velocity vector of a liquid particle at the free surface is $\boldsymbol{u}$. Hence the impermeability condition takes the form

$$u+\frac{\partial f}{\partial t}+\frac{\partial f}{\partial z}w=0. \tag{18}$$

For the derivative in the direction of the free surface we get from (18)

$$\frac{\partial u}{\partial z}-\frac{\partial f}{\partial z}\frac{\partial u}{\partial r}+\frac{\partial^2 f}{\partial z\,\partial t}+\frac{\partial^2 f}{\partial z^2}w+\frac{\partial f}{\partial z}\left(\frac{\partial w}{\partial z}-\frac{\partial f}{\partial z}\frac{\partial w}{\partial r}\right)=0. \tag{19}$$

Substitution of (8), (15), (16) and (17) into (18) yields the impermeability condition at the free surface with respect to the functions to be determined:

$$\frac{\partial \psi}{\partial z}+(b-f)\frac{\partial f}{\partial t}-\frac{\partial f}{\partial z}\frac{\partial \psi}{\partial r}=0. \tag{20}$$

Next we have to consider the equilibrium of stresses at the free surface. This condition is given by (see, e.g. Landau & Lifshitz 1987)

$$\boldsymbol{\sigma}\cdot\boldsymbol{n}=T_{12}2H\boldsymbol{n}, \tag{21}$$

where $\boldsymbol{\sigma}$ denotes the stress tensor, T_{12} the liquid/gas surface tension coefficient (assumed to be constant), and H the mean curvature of the free surface. The components of the stress tensor in cylindrical coordinates may be found in most textbooks on fluid mechanics (e.g. Landau & Lifshitz 1981, p. 48) and thus are omitted.

For fluid configurations with rotational symmetry we obtain for twice the value of the mean curvature

$$2H=-\left[\frac{1}{b-f}\left\{1+\left(\frac{\partial f}{\partial z}\right)^2\right\}^{-1/2}+\frac{\partial^2 f}{\partial z^2}\left\{1+\left(\frac{\partial f}{\partial z}\right)^2\right\}^{-3/2}\right]. \tag{22}$$

Multiplication of (21) with the tangent vector

$$\boldsymbol{t}=\frac{-1}{[1+(\partial f/\partial z)^2]^{1/2}}\left(\frac{\partial f}{\partial z},0,1\right)^T \tag{23}$$

yields the differential equation

$$2\frac{\partial f}{\partial z}\left(\frac{\partial u}{\partial r}-\frac{\partial w}{\partial z}\right)-\left[1-\left(\frac{\partial f}{\partial z}\right)^2\left(\frac{\partial w}{\partial r}+\frac{\partial u}{\partial z}\right)\right]=0 \tag{24}$$

for the stress balance in the axial-tangential direction. Furthermore, we get for the stress balance in the transverse direction

$$\frac{\partial v}{\partial r}-\frac{v}{r}+\frac{\partial f}{\partial z}\frac{\partial v}{\partial z}=0. \tag{25}$$

As an additional equation we employ the radial component of (21). In dimensionless form this equation reads

$$p-Ek\left[2\frac{\partial u}{\partial r}+\frac{\partial f}{\partial z}\left(\frac{\partial w}{\partial r}+\frac{\partial u}{\partial z}\right)\right]=\frac{2H}{We}, \tag{26}$$

where $We=\rho L^3\Omega^2/T_{12}$ is the Weber number. Employing (8) gives for the balance of the normal stresses (26) and the balance of the axial-tangential stresses (24)

$$p-Ek\left[2\left(\frac{1}{r^2}\frac{\partial\psi}{\partial z}-\frac{1}{r}\frac{\partial^2\psi}{\partial r\,\partial z}\right)+\frac{\partial f}{\partial z}\left(-\frac{1}{r^2}\frac{\partial\psi}{\partial r}+\frac{1}{r}\frac{\partial^2\psi}{\partial r^2}-\frac{1}{r}\frac{\partial^2\psi}{\partial z^2}\right)\right]=\frac{2H}{We}, \tag{27}$$

and

$$2\frac{\partial f}{\partial z}\left(\frac{\partial\psi}{\partial z}-2r\frac{\partial^2\psi}{\partial r\,\partial z}\right)-\left(1-\left(\frac{\partial f}{\partial z}\right)^2\right)\left[-\frac{\partial\psi}{\partial r}+r\left(\frac{\partial^2\psi}{\partial r^2}-\frac{\partial^2\psi}{\partial z^2}\right)\right]=0, \tag{28}$$

respectively.

To eliminate the pressure in the balance equation for the normal stresses, (27) can be differentiated in the direction of the free surface and accordingly combined with the Navier–Stokes equations in the radial and axial directions. Thus

$$r\frac{\partial\psi}{\partial z}\frac{\partial^2\psi}{\partial r\,\partial z}-r\frac{\partial^2\psi}{\partial z^2}\frac{\partial\psi}{\partial r}-r^2\frac{\partial^2\psi}{\partial z\,\partial t}-\left(\frac{\partial\psi}{\partial z}\right)^2-r^4-2r^3v-r^2v^2$$
$$=-r^3\frac{\partial p}{\partial r}+Ek\left(r\frac{\partial^2\psi}{\partial r\,\partial z}-r^2\frac{\partial^3\psi}{\partial r^2\,\partial z}r-{}^2\frac{\partial^3\psi}{\partial z^2}\right), \tag{29}$$

and

$$r\frac{\partial\psi}{\partial r}\frac{\partial^2\psi}{\partial r\,\partial z}+r^2\frac{\partial^2\psi}{\partial r\,\partial t}-r\frac{\partial\psi}{\partial z}\frac{\partial^2\psi}{\partial r^2}+\frac{\partial\psi}{\partial z}\frac{\partial\psi}{\partial r}$$
$$=-r^3\frac{\partial p}{\partial z}+F_z r^3+Ek\left(r^2\frac{\partial^3\psi}{\partial r\,\partial z^2}+r^2\frac{\partial^3\psi}{\partial r^3}-r\frac{\partial^2\psi}{\partial r^2}+\frac{\partial\psi}{\partial r}\right). \tag{30}$$

Finally we have to formulate a contact line condition. Since for a moving contact line the no-slip condition leads to infinitely high stresses, we postulate that in the (r, z)-plane the stresses vanish at the contact line, otherwise the no-slip condition (adherence condition) holds. This leads to the following boundary conditions between the free liquid surface and the vessel wall at the contact line.

Since the contact lines are located at the plane surfaces (solid end plates) of the cylinder, the velocity normal to the wall must vanish (12*c*). Likewise $\partial w/\partial r=0$. Considering the (r, z)-stress component $\sigma_{rz}=\eta(\partial w/\partial r+\partial w/\partial z)$ with $\eta=\nu\rho$ the dynamic viscosity of the liquid, it follows from the stream function–vorticity equation that $\omega=0$.

In addition, putting the stress components σ'_{rr} and σ'_{zz} (these are the stress components without the pressure part; cf. Landau & Lifshitz 1978) equal to zero it results from (19) that

$$\frac{\partial^2 f}{\partial z\,\partial t}=0. \tag{31}$$

This is identical with the assumption that the dynamic contact angle is equal to the static contact angle.

3. Numerical treatment of the problem

3.1. *Transformation to surface-adapted coordinates*

For the numerical solution of the problem we utilize a grid, the upper grid line of which is a coordinate line of the free surface. A possible coordinate transformation is shown in figure 2. The transformation reads

$$\tau = t, \quad \zeta = z, \quad \xi = \frac{b-r}{f(z,t)}, \tag{32a–c}$$

with τ as the time, and ζ and ξ as the axial and radial coordinates in the new coordinate system, respectively. The new variable ξ is defined in such a way that its value at the free surface is one (independent of z) and its value at the lateral area is zero. Thus, employing the extended chain rule the first derivatives of an arbitrary function $g(\xi, \zeta, \tau)$ in the non-transformed system are

$$\frac{\partial g}{\partial r} = -\frac{1}{f}\frac{\partial g}{\partial \xi}, \quad \frac{\partial g}{\partial z} = -\frac{\xi}{f}\frac{\partial f}{\partial \zeta}\frac{\partial g}{\partial \xi} + \frac{\partial g}{\partial \zeta}, \quad \frac{\partial g}{\partial t} = -\frac{\xi}{f}\frac{\partial f}{\partial \tau}\frac{\partial y}{\partial \xi} + \frac{\partial g}{\partial \tau}, \tag{33a–c}$$

Higher derivatives can be generated by successive differentiation of the derivatives of lower order. Since the transformation of the differential equations will be performed using REDUCE, neither the higher derivatives nor the transformed differential equations will be stated here. Further details are documented by Ehmann (1991).

3.2. *The spectral Galerkin method*

In connection with the numerical investigation, only periodic solutions are studied without consideration of the initial conditions, i.e. in this work the transient state is not dealt with. The fundamental equations set out in §2 are solved approximately in the time direction (τ) by means of the Galerkin method, using set-up functions which correspond to the first terms of a Fourier series. Thereupon the resulting system of differential equations depends on ξ and ζ only. These equations are then approximated using the finite difference method, which gives a nonlinear system of equations for the determination of the discrete flow quantities.

Generally the differential equations can be cast into the form

$$L_p(g_q(\boldsymbol{x}, t)) = 0, \tag{34}$$

where L_p denotes the differential operators of the differential equations and g_q the required functions. The points of the physical space $D(\boldsymbol{x})$, where the differential equations have to be fulfilled, are denoted by $\boldsymbol{x}$. The boundary conditions at the boundary ∂D are given by

$$\Lambda_s(g_q(\boldsymbol{x}, t)) = 0, \tag{35}$$

where Λ_s denotes the differential operators of the boundary conditions. For the approximate solution of the problem formulated by (34) and (35) we put

$$g_{q_a} = \sum_{k=-K}^{K} A_{q_k}(\boldsymbol{x})\, \Phi_{q_k}(t), \tag{36}$$

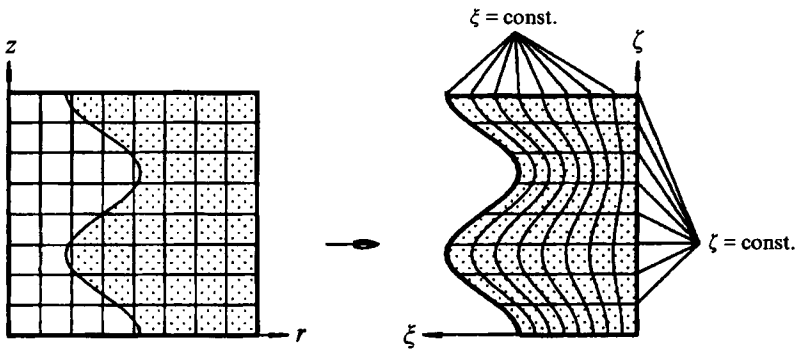

FIGURE 2. Representation of the coordinate transformation.

where the A_{q_0} are functions which satisfy the boundary conditions and where the spectral set-up (complex Fourier series)

$$A_{q_{-k}}(x) = \overline{A_{q_k}(x)}, \quad \Phi_{q_k}(t) = \mathrm{e}^{\mathrm{i}\Omega_A kt} \tag{37}$$

has been employed. The conjugate is denoted by an overbar. The $\Phi_{q_k}(t)$ are known analytic functions (set-up functions) of time, taking into account (32*a*), and the unknown coefficients A_{q_k} depend on the position x only. Substitution of (36) into (34) yields for the pth differential equation the residue

$$R_p = L_p\Big(\sum_{k=-K}^{K} A_{q_k}(x)\,\Phi_{q_k}(t)\Big). \tag{38}$$

According to the method of weighted residues (MWR) – and the Galerkin method is such a procedure – we determine the $A_{q_k}(x)$ by setting

$$R_{p_l} = \int_{t_0}^{t_0+(2\pi/\Omega_A)} R_p\,\mathrm{e}^{\mathrm{i}\Omega_A lt}\,\mathrm{d}t = 0. \tag{39}$$

This is a system of equations for the coefficients $A_{q_k}(x)$ of the set-up functions. In our case the time interval is the oscillation period $(2\pi/\Omega_A)$ and integration with respect to time can be carried out analytically.

3.3. *Discretization in the space direction*

For the spatial discretization a finite difference approximation is applied. In doing so only computational molecules (difference stars) with a truncation (discretization) error of at least the second order are utilized. Moreover the computational molecules at the walls are adapted to the boundary conditions. To describe the flow in domains of possible boundary layers properly, the mesh management has to take into consideration refined grids. For this purpose grids with an exponential distribution are advantageous. Moreover, to avoid a degradation of the truncation error in the domains of the refined grid, the latter is transformed on an equidistant grid (see Anderson, Tannehill & Pletcher 1984). Thereby new coordinates are again introduced which correspond to the counting variables of the grid. They are x in the ξ-direction and y in the ζ-direction; thus the transformation law is given by

$$x = x(\xi), \quad y = y(\zeta). \tag{40*a*, *b*}$$

Application of the chain rule yields the derivatives from the non-transformed rectangular coordinate system $(\xi-\zeta)$. These formulae, however, are not reproduced here (cf. Ehmann 1991).

According to Anderson *et al.* (1984) the derivatives used within the now equidistant grid can be approximated by central differences. Thus

$$\left.\frac{\partial g}{\partial x}\right|_{i,j} = \frac{g_{i,j+1}-g_{i,j-1}}{2}, \quad \left.\frac{\partial g}{\partial y}\right|_{i,j} = \frac{g_{i+1,j}-g_{i-1,j}}{2}, \tag{41a, b}$$

$$\left.\frac{\partial^2 g}{\partial x^2}\right|_{i,j} = g_{i,j+1}+g_{i,j-1}-2g_{i,j}, \quad \left.\frac{\partial^2 g}{\partial y^2}\right|_{i,j} = g_{i+1,j}+g_{i-1,j}-2g_{i,j}. \tag{42a, b}$$

and for the mixed second derivative

$$\left.\frac{\partial^2 g}{\partial x\,\partial y}\right|_{i,j} = \tfrac{1}{4}(g_{i+1,j+1}+g_{i-1,j-1}-g_{i+1,j-1}-g_{i-1,j+1}). \tag{43}$$

In these formulae the indices i and j denote the counting variables of the grid in the x- and y-directions, respectively.

Derivatives of the third order can be determined by means of Taylor series, but their representation will be omitted here. However, it should be pointed out that the first derivatives can lead to undesirable waves, if the problem is not dominated by terms with second derivatives. These waves arise because of a weak coupling between neighbouring grid points. To avoid this phenomenon, asymmetric computational molecules will be used, e.g. at the interface (free surface) the first derivative in ξ-direction reads

$$\left.\frac{\partial g}{\partial x}\right|_{i,J} = \tfrac{1}{3}g_{i,J+1}+\tfrac{1}{2}g_{i,J}-g_{i,J-1}+\tfrac{1}{6}g_{i,J-2}, \tag{44}$$

since the computational molecules at the free surface protude beyond the free surface by one grid point.

4. Discussion of results

4.1. *The eigenvalue equation*

Since the objective of the present investigation is the periodic response of a rotating liquid annulus as a result of a periodic axial excitation, in particular in the range of the eigenfrequencies, it is necessary to determine these frequencies. Thereby the eigenmodes are defined in such a way that the order of the eigenmode corresponds to the number of nodes of a standing wave. As shown by Raake (1991), only odd eigenmodes are generated in the axial direction, owing to periodicity and symmetry.

In order to exemplify and to facilitate the numerical investigation within the frequency ranges of the eigenmodes, it is advantageous to utilize a frequency equation due to Bauer (1982*a*,*b*). This equation is based on a linearized, inviscid theory for a two-phase immiscible fluid system and yields two frequency ranges: the hyperbolic range ($\hat{\omega} < 2\Omega$), and the elliptic range ($\hat{\omega} > 2\Omega$), where $\hat{\omega}$ is the eigenfrequency, and 2Ω twice the angular speed of the rotating cuvette. In the hyperbolic case solutions exist with a distinct number of radial nodes, while in the elliptic case no radial nodes exist.

Because in our case the density ratio of the inner to the outer fluids vanishes and because of the assumed rotational symmetry, only eigenvalues of zeroth order in the axial direction are determined. Therefore, Bauer's frequency equation reduces to

$$\theta J_0'(\theta)\left\{\mp k\theta X Y_0(k\theta)\,J_0'(k\theta)-\frac{1}{4}\left[-1+\frac{T_{12}}{\rho a^3\Omega^2 k^3}(1-k^2\gamma)\right](1\pm X)\,(k\theta)^2 J_0'(k\theta)\,Y_0'(k\theta)\right\}$$

$$+k\theta^2 J_0'(k\theta)\,Y_0'(\theta)\left\{\tfrac{1}{4}(1+X)\,k\theta\left[-1+\frac{T_{12}}{\rho a^3\Omega^2 k^3}(1-k^2\gamma)\right]J_0'(k\theta)\pm X J_0'(k\theta)\right\}=0, \tag{45}$$

with $$k = b/a, \quad \gamma = (n\pi a/h)^2, \quad X = \theta^2/\gamma. \tag{46}$$

The upper sign in (45) corresponds to the hyperbolic case, the lower sign to the elliptic case; n is the number of nodes in the axial direction. J_0 and Y_0 are the Bessel functions of zeroth order, of the first and second kind, respectively. A prime denotes differentiation. With respect to the elliptic case the Bessel functions J_0 and Y_0 must be replaced by I_0 and K_0, where I_0 and K_0 are the modified Bessel functions of zeroth order and the second kind, respectively.

If solutions for θ are found, the eigenfrequencies can be calculated from

$$\frac{\hat{\omega}^2_{mn\lambda}}{4\Omega^2} = \begin{cases} \dfrac{1}{1+\theta^2_{mn\lambda}/\gamma} < 1, & \text{hyperbolic case,} \\ \dfrac{1}{1-\theta^2_{mn\lambda}/\gamma} > 1, & \text{elliptic case,} \end{cases} \tag{47a, b}$$

where the numbers m, n and λ designate the revolving ($m = 0$), the longitudinal (n), and the radial (λ) oscillation modes, respectively.

4.2. *Eigenmode of the first order in the axial direction with one and two radial nodes*

Since the behaviour of the flow subject to an excitation by an eigenfrequency in the hyperbolic range of the linearized inviscid flow theory is of special interest, the temporal development of the flow pattern will be described in the following in some detail. For the numerical experiment typical physical data for fluids are used, and the cylinder has a diameter of 4 cm and a height of 4 cm and is filled such that the steady free surface of the rotating fluid is located at the semi-radius of the cuvette. For that configuration the input data are

$$Ek = 6.250 \times 10^{-5}; \quad We = 2.133 \times 10^4; \quad b = 0.5; \quad f = 0.25,$$

where the angular speed of the revolving cuvette is 10^{-1} s. If one is interested in the first eigenfrequency in the axial direction one notes, along with the solution of the eigenfrequency equation, that the hyperbolic case occurs. There are no eigenfrequencies with one axial node, the dimensionless frequency of which is $\omega_0 > 2$. Thus it seems particularly interesting to demonstrate the appearance of radial nodes. The application of an equidistant grid yielded absurd results. For example in the case of the transverse velocities waves occur with a wavelength that corresponds to twice the distance between two adjoining grid points. According to Gresho & Lee (1981) this phenomenon is possibly due to thin boundary layers having a thickness smaller than the grid distance. Hence an exponential refinement of the grid at the walls is utilized as mentioned previously. Thereby 50 grid points in the radial direction and 80 grid points in the axial direction are employed, where a domain of thickness $\delta = 0.1$ with a refined grid was taken as a basis. This domain proceeds from fixed boundaries in such a way that in the lateral area there are 10 points, while at the plane front plates there are 20 grid points. Figure 3 shows the development of the flow pattern for an excitation with a frequency $\hat{\omega} = 0.395$, corresponding to the solution of the eigenfrequency equation.

Flow pictures for increasing time are plotted over the semiperiod of the oscillation. The second half of the oscillation period is then obtained by reflection of the pictures in the symmetry plane which is perpendicular to the axis of revolution. A picture produced by reflection in this way is assigned to a point of time shifted by a half-period.

For a better ordering of the flow configurations within the oscillation period a new dimensionless time $\tilde{t}$ was introduced related to the old dimensionless time by $\tilde{t} = \Omega_A t$.

On the upper left-hand side of each of figures 3(*a*) to 3(*e*) the rotating cuvette is

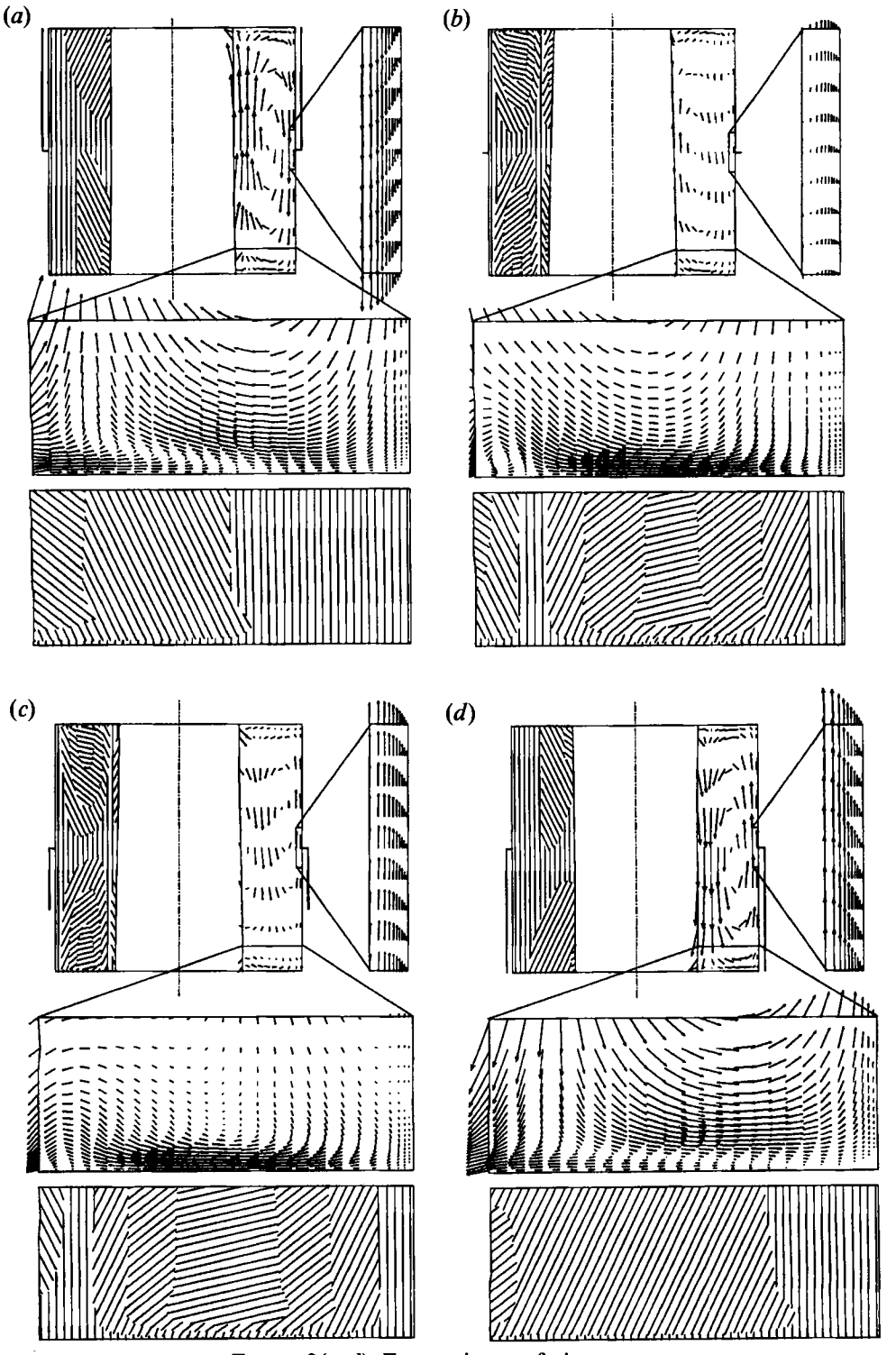

FIGURE 3(*a–d*). For caption see facing page.

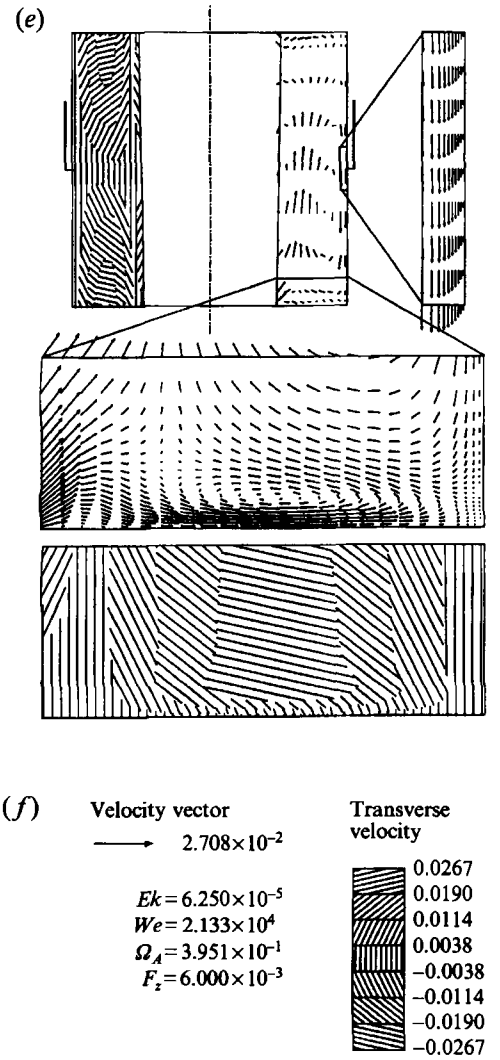

FIGURE 3. Sequence of an eigenmode with radial nodes at times (*a*) $\bar{t} = 0$, (*b*) 1.571, (*c*) 2.094, (*d*) 3.142, (*e*) 5.236. (*f*) Legend for the velocity vector and transverse velocity fields.

shown, with the velocity field about the symmetry line (relative transverse velocity) at the left, corresponding to the legend in figure 3(*f*), and the velocity components in the (r, z)-plane at the right in the form of velocity vectors. On the left and the right of each cuvette the instantaneous volume force resulting from the axial acceleration of the container is marked by a bar in the corresponding direction. The maximal value of this force is $F_z = 6.000 \times 10^{-3}$. To the right of the cuvette an enlarged sector of a small domain of the lateral area is shown for a better representation of the flow near the walls. The position of the magnified area is framed in the general view. Below these representations the boundary layer domain at the end planes is shown magnified, first the velocities in the (r, z)-plane, and, beneath, the transverse velocities in this domain. It should be noticed that here the magnification corresponds to the flow field to the right of the axis of rotation, and so both representations of the transverse velocities appear reflected.

Starting the discussion of the flow pattern at the time $\tilde{t} = 0$, one recognizes a radial node by observing a reversing of the velocities in the axial direction at a line. At the same time the free surface at the upper plane moves towards the symmetry line of the container, while at the lower plane the free surface moves away from the symmetry line. In the axial direction a node can be determined in such a way that there exists only one point at the interface where the velocities in the radial direction reverse.

Examination of the flow configuration development with time shows a decrease of the velocities until, eventually, two radial nodes occur at the moment $\tilde{t} = 1.571$. Thus there are two lines within the fluid where the direction of the axial components of the velocities reverse. This is only possible if these two eigenfrequencies are excited. But this means, however, that they occur as immediately adjacent eigenfrequencies. This is confirmed by inspection of the zeros of the eigenvalue equation, since the eigenvalues for the first and second eigenfrequencies with one axial node only are $\hat{\omega} = 0.4011$ and $\hat{\omega} = 0.3951$, respectively. The fact that the appropriate eigenmodes become visible at different moments results from a phase difference, because the difference between the excitation frequency and the eigenfrequencies is large.

Subsequently the first eigenmode becomes dominant again until, finally, at $\tilde{t} = 3.142$, a flow pattern results which corresponds to a reflection of the flow pattern at the time $\tilde{t} = 0$ at the equatorial plane of the cylinder. Following this the second half of the period is traversed.

Consideration of the velocity fields of the transverse velocities suggests a clear connection between the radial velocity component and the Coriolis acceleration, such that in domains where the radial component is directed outward, the fluid in the transverse direction is subject to a negative acceleration, while a radial component directed inward exerts a positive acceleration effect on the transverse velocity component.

The velocity field in the lateral area at all times decreases towards that area due to the adherence condition. Here, it must be taken into account that there is no steady flow. Thus phase shifts due to damping may appear in the boundary layer domain. It should also be noticed that the domain of the eigenmodes varies. Hence the definition of the boundary layer thickness is difficult, particularly since the latter changes periodically during the development of the flow field.

Next the velocities at the bottom of the cuvette are discussed. In particular a backflow region near the wall at time $\tilde{t} = 0$ is noticeable, the thickness of which decreases in the outward direction until it disappears completely. During the subsequent development the fluid in the backflow region is entrained more and more by the flow within the interior of the fluid. Hence the end of the backflow region is continually transported further inward until eventually at time $\tilde{t} = 2.094$ the entire backflow region has disappeared. It should be pointed out that the flow between the domain dominated by the eigenmode and the wall shows a strongly marked maximum in the axial direction. An explanation for this is that it results from damping and in addition from the influence of the wall on the transversal velocity. Both cause a phase shift that can explain the described behaviour.

The flow pattern at $\tilde{t} = 2.094$ reveals that a new backflow region originates in which the velocities in the interior of the fluid reverse corresponding to the eigenmode. Later this backflow region is again transported from the exterior in the direction of the free surface of the fluid until finally it vanishes at time $\tilde{t} = 5.236$.

With respect to the transverse velocities displayed, their decrease in the direction of the wall is seen on one side, and the connection between the Coriolis acceleration and the radial component of the velocities is seen on the other side.

5. Conclusions

We have presented a numerical method to examine a problem with a free surface using a coordinate system adapted to the surface. Since only the periodic response of a rotating liquid annulus subject to an axial harmonic excitation in the range of an eigenfrequency was studied, spectral methods were applied in the time direction. In the space direction a discrete approximation via the method of finite differences was utilized. The computer program was produced to some extent from a program for the processing of symbolic data. Numerical results demonstrated good agreement with analytical predictions based on a linearized inviscid flow theory. Furthermore interesting insights could be acquired regarding the formation of boundary layers. Such flow phenomena, however, cannot be explained by means of a non-viscous flow theory.

The authors are indebted to the referees for helpful and constructive comments.

REFERENCES

ANDERSON, D. A., TANNEHILL, J. C. & PLETCHER, R. H. 1984 *Computational Fluid Mechanics and Heat Transfer*. Hemisphere.

BALASUBRAMANIAN, R. 1990 Numerical simulation of unsteady viscous free surface flow. *J. Comput. Phys.* **90**, 396–430.

BAUER, H. F. 1980 Schwingungen nichtmischbarer Flüssigkeiten im rotierenden Kreiszylinder. *Z. Angew. Math. Mech.* **60**, 653–661.

BAUER, H. F. 1981 Freie Schwingungen nichtmischbarer Flüssigkeiten im rotierenden Kreiszylinder unter Berücksichtigung der Oberflächenspannung. *Forsch. Ing.-Engng Res.* **47** (6), 190–198.

BAUER, H. F. 1982*a* Rotating finite liquid systems under zero-gravity. *Forsch. Ing.-Engng Res.* **48** (6), 169–200.

BAUER, H. F. 1982*b* Coupled oscillations of a solidly rotating liquid bridge. *Acta Astronautica* **9**, 547–563.

BAUER, H. F. 1984 Natural damped frequencies of an infinitely long column of immiscible viscous liquids. *Z. Angew. Math. Mech.* **64**, 475–490.

BECKER, E. & BÜRGER, W. 1975 *Kontinuumsmechanik*. Teubner.

CANUTO, C., HUSSANINI, M. Y., QUARTERONI, A. & ZANG, T. A. 1988 *Spectral Methods in Fluid Dynamics*. Springer.

CARRUTHERS, R. J. & GRASSO, M. 1972 Studies of floating liquid zones in simulated zero gravity. *J. Appl. Phys.* **43**, 436–445.

CHUN, CH.-H., EHMANN, M., SIEKMANN, J. & WOZNIAK, G. 1987 Vibrations of rotating menisci. In *Proc. 6th European Symp. on Materials Sciences under Microgravity Conditions, Bordeaux, France, February 1987*, ESA-256, pp. 226–234.

DALY, B. J. 1969 Technique for including surface-effects in hydrodynamic calculations. *J. Comput. Phys.* **4**, 97–117.

EHMANN, M. 1991 Numerische Berechnung der Schwingungen axial angeregter rotationssymmetrischer Flüssigkeitsannuli in rotierenden zylindrischen Behältern. Dissertation, Universität GH Essen.

FLETCHER, C. A. J. 1984 *Computational Galerkin Methods*. Springer.

GILLIS, J. 1961 Stability of a column of rotating viscous liquid. *Proc. Camb. Phil. Soc.* **57**, 152–159.

GREENSPAN, H. P. 1969 *The Theory of Rotating Fluids*. Cambridge University Press.

GRESHO, P. M. & LEE, R. L. 1981 Don't suppress the wiggles – they're telling you something! *Computers Fluids* **9**, 223–253.

HARLOW, F. H. & WELCH, J. E. 1965 Numerical calculation of time-dependent viscous incompressible flow of fluid with free surface. *Phys. Fluids* **8**, 2182–2189.

HEARN, A. C. 1983 *REDUCE User's Manual*, Version 3.0. Rand Publication CP78.

HIRT, C. W., AMSDEN, A. A. & COOK, J. L. 1974 An arbitrary Lagrangian–Eulerian computing method for all flow speeds. *J. Comput. Phys.* **14**, 227–253.

HIRT, C. W. & NICHOLS, B. D. 1981 Volume of fluid (VOF) method for the dynamics of free boundaries. *J. Comput. Phys.* **39**, 201–225.

HOCKING, L. M. 1960 The stability of a rigidly rotating column of liquid. *Mathematika* **1** (7), 1–9.

HOCKING, L. M. & MICHAEL, D. H. 1959 The stability of a column of a rotating liquid. *Mathematika* **25** (6), 25–32.

HULZEN, VAN J. A. & CALMET, J. 1982 Computer algebra systems. In *Computer Algebra Symbolic and Algebraic Computation* (ed. B. Buchberger, G. E. Collins & R. Loos, in cooperation with R. Albrecht). Springer.

KOLLMANN, F. G. 1962 Freie Schwingungen eines rotierenden Flüssigkeitsringes. *Ing. Arch.* **XXXI**, 250–257.

LANDAU, L. D. & LIFSCHITZ, E. M. 1987 *Fluid Mechanics*, 2nd end. Pergamon.

MASON, G. 1970 An experimental determination of the stable length of cylindrical liquid bubbles. *J. Colloid Interface Sci.* **32**, 172–176.

MILES, J. W. 1959 Free surface oscillations in a rotating liquid. *Phys. Fluids* **2**, 297–305.

MILES, J. W. & TROESCH, B. A. 1961 Surface oscillations of a rotating liquid. *J. Appl. Mech.* **83**, 491–496.

PEYRET, R. & TAYLOR, TH. D. 1983 *Computational Methods for Fluid Flow*. Springer.

PLATEAU, J. A. F. 1873 *Statique Expérimentale et Théorique des Liquides Soumis aux Seules Forces Moléculaires*. Gauthier-Villars.

RAAKE, D. 1991 Untersuchung axial erregter Eigenschwingungen nichtmischbarer Fluide in einer schnell rotierenden zylindrischen Küvette. Dissertation, Universität GH Essen.

RAYLEIGH, LORD 1892 On the instability of cylindrical fluid surfaces. *Phil. Mag.* (5) **34**, 177–180.

RAYNA, G. 1987 *REDUCE Software for Algebraic Computation*. Springer.

RYSKIN, G. & LEAL, L. G. 1984 Numerical solution of free-boundary problems in fluid mechanics. Part 1. The finite-difference technique. *J. Fluid Mech.* **148**, 1–17.

SEEBOLD, J. G. & REYNOLDS, W. C. 1965 Configuration and stability of a rotating axisymmetric meniscus at low g. Tech. Rep. LG-4. Thermosciences Division, Department of Mechanical Engineering, Stanford University.

VELDMAN, A. E. P. & VOGELS, M. E. S. 1984 Axisymmetric liquid sloshing under low-gravity conditions. *Acta Astronautica* **11**, 641–649.